Life Sciences 231 (2019) 116559

Contents lists available at ScienceDirect

Life Sciences

journal homepage: www.elsevier.com/locate/lifescie

Lack of zinc finger protein 521 upregulates dopamine β-hydroxylase expression in the mouse brain, leading to abnormal behavior

Nobutaka Ohkubo*, Mamoru Aoto, Kazunori Kon, Noriaki Mitsuda

Department of Circulatory Physiology, Graduate School of Medicine, Ehime University, Shitsukawa, Toon, Ehime 791-0295, Japan.

ARTICLE INFO

Keywords:
Zinc finger protein 521
Dopamine
Noradrenaline
Behavior
Dopamine beta-hydroxylase
Schizophrenia

ABSTRACT

Aim: Previously, we reported that mice deficient in most of the *Zfp521* coding region (*Zfp521*$^{\Delta/\Delta}$ mice) displayed abnormal behaviors, including hyperlocomotion and lower anxiety. In this study, we aimed to elucidate the involvement and mechanisms of monoamine variation.

Main methods: First, we compared the levels of dopamine (DA), noradrenaline (NA), and serotonin in the brains of *Zfp521*$^{\Delta/\Delta}$ and *Zfp521*$^{+/+}$ mice using enzyme-linked immunosorbent assay. Next, we elucidated the mechanisms using quantitative PCR and Western Blotting. Additionally, we administered inhibitory drug to the mice and performed behavioral tests.

Key findings: Our results showed that the DA level decreased and the NA level increased in *Zfp521*$^{\Delta/\Delta}$ mice. We found that ZFP521 suppresses the expression of dopamine β-hydroxylase (DBH), which converts DA into NA. We also demonstrated that paired homeodomain transcription factor 2 and early growth response protein-1, which are the transcription factors for *Dbh*, were involved in the upregulation of *Dbh* by ZFP521. The administration of nepicastat, a specific inhibitor of DBH, attenuated the abnormal behaviors of *Zfp521*$^{\Delta/\Delta}$ mice.

Significance: These results suggest that the lack of ZFP521 upregulates the expression of DBH, which leads to a decrease in the DA level and an increase in the NA level in the brain, resulting in abnormal behaviors.

1. Introduction

Zinc finger protein 521 (ZFP521) is a transcriptional regulatory factor with 30 Krüppel-like zinc finger motifs and a nuclear localization signal [1]. In mice, ZFP521 is ubiquitously expressed in the whole body, with an especially high expression in the brain [2]. Although the exact role of ZFP521 in the brain remains unclear, Kamiya et al. suggested that it serves as a switch for neural stem cell differentiation during development [3]. They also reported that the suppression of ZFP521 inhibited differentiation from epiblast cells into neuroectodermal stem cells, even when differentiation was induced. By contrast, overexpression of ZFP521 promoted differentiation into neuroectodermal stem cells [3]. In the embryonic brain, ZFP521 has been shown to promote the proliferation and differentiation of neurons in the striatum [4]. In the adult brain, *Zfp521* is expressed in the hippocampus and striatum [5]. In the striatonigral region of the adult brain, ZFP521 seems to interact and to be inhibited by early B-cell factor 1 (EBF1), which is important for the development of spiny neurons [4].

Previously, we generated mice deficient in most of the *Zfp521* coding region (*Zfp521*$^{\Delta/\Delta}$ mouse). We then analyzed their behaviors using methods like the open field test and elevated plus maze test, which revealed that *Zfp521*$^{\Delta/\Delta}$ mice had a hyperlocomotive action and lower anxiety levels compared to *Zfp521*$^{+/+}$ mice [5]. However, the mechanisms underlying these abnormal behaviors due to *Zfp521* mutation were unknown.

Monoamine neurotransmitters, such as dopamine (DA), noradrenaline (NA), and serotonin (5-HT), can greatly impact animal behavior. For example, DA or its receptor deficiency in mice results in chronic depression and anxiety [6]. It has also been reported that the motor activity correlates with the cortical levels of DA and NA [7]. Colomba mice exhibit hyperactivity locomotor and an imbalance in catecholamine regulation, in which brain DA reduced, whereas NA concentrations are considerably increased [8].

In the present study, we compared the levels of DA, NA, and 5-HT in the brains of *Zfp521*$^{\Delta/\Delta}$ and *Zfp521*$^{+/+}$ mice. We then investigated the mechanism of monoamine regulation by ZFP521 using cultured cells transfected with *Zfp521* expression vectors or siRNA.

* Corresponding author.
E-mail address: nobu@m.ehime-u.ac.jp (N. Ohkubo).

https://doi.org/10.1016/j.lfs.2019.116559
Received 7 March 2019; Received in revised form 22 May 2019; Accepted 10 June 2019
Available online 11 June 2019

2. Materials and methods

2.1. Reagents

2-CAT (N-D) and serotonin enzyme-linked immunosorbent assay (ELISA) kits were purchased from Labor Diagnostika Nord GmbH and Co. (Nordhorn, Germany). DNA oligonucleotides as primers for real-time polymerase chain reaction [quantitative PCR (qPCR)] were synthesized and purchased from Sigma-Aldrich (St. Louis, MO, USA). Rabbit anti-ZFP521 (ZNF521) polyclonal antibody was purchased from ProteinExpress Co., Ltd. (Chiba, Japan), rabbit anti-dopamine β-hydroxylase polyclonal antibody from ImmunoStar (Hudson, WI, USA), rabbit anti-PHOX2A polyclonal antibody from ProSci Incorporated (Poway, CA, USA), rabbit anti-EGR-1 monoclonal antibody from Cell Signal Technology (Boston, MA, USA), rabbit anti-P300 polyclonal antibody from Santa Cruz Biotechnology (Santa Cruz, CA, USA), rabbit anti-β-actin polyclonal antibody from FUJIFILM Wako Pure Chemical (Osaka, Japan), rabbit anti-tyrosine hydroxylase polyclonal antibody from Cell Signaling Technology, HRP conjugated anti-rabbit IgG polyclonal antibody from Promega (Madison, WI, USA), and Alexa Fluor 568-conjugated anti-rabbit IgG antibody from Thermo Fisher Scientific (Rockford, IL, USA). *Zfp521* siRNA and scrambled control siRNA were purchased from Sigma-Aldrich. Mammalian expression vector pCMV6 containing mouse *Zfp521* full-length cDNA was purchased from OriGene Technologies (Rockville, MD, USA). Polyethyleneimine (PEI) max was purchased from Polysciences Inc. (Warrington, PA, USA). Nepicastat hydrochloride was purchased from Sigma-Aldrich. All other reagents were purchased from FUJIFILM Wako Pure Chemical.

2.2. Animals

All mice were housed in a specific pathogen-free facility under a 12 h light/dark cycle with ad libitum access to water and a regular diet. $Zfp521^{\Delta/+}$ mice were crossed to obtain $Zfp521^{\Delta/\Delta}$ mice, and littermate $Zfp521^{+/+}$ mice were used as controls. The mice were routinely genotyped as described previously [5]. Male $Zfp521^{\Delta/\Delta}$ mice (5–8 week-old; weight approximately 10 g) and age-matched, sex-matched $Zfp521^{+/+}$ mice (5–8 week-old; weight approximately 20 g) were used for behavioral studies or brain samples' collection. The protocol for *ZFP521* mutant mice studies was approved by the Institutional Review Board of Ehime University Graduate School of Medicine (Permit no. 05-SO-38-16). All animal studies were carried out in accordance with the guidelines of the Ehime University School of Medicine Committee on Animals. All surgeries were performed under anesthesia with the administration of midazolam (4 mg/kg BW), medetomidine hydrochloride (0.3 mg/kg BW), and butorphanol tartrate (5 mg/kg BW). All efforts were made to minimize suffering.

2.3. Cell culture and transfection

Murine neuroblastoma neuro-2a cells were maintained in Dulbecco's modified Eagle's medium (DMEM; Wako Pure Chemicals) supplemented with 10% fetal bovine serum (FBS) with penicillin-streptomycin solution (FUJIFILM Wako Pure Chemical) in a humidified 5% CO_2 environment at 37 °C. Rat pheochromocytoma (PC12) cells were maintained in DMEM supplemented with 10% FBS and 5% horse serum with penicillin-streptomycin solution in a humidified 5% CO_2 environment at 37 °C.

Cells were precultured for 16 h in DMEM containing 1% FBS in 12-well plates (1.5×10^5 cells/mL). After preculture, pCMV6 vector or siRNA was added to the cell culture supernatant using PEI max. After four hours of transfection, the medium was removed and replaced with a fresh medium.

2.4. Measurement of monoamine levels

For cell culture, 1 μM of ascorbic acid and 55 mM of potassium chloride were added to the PC12 cell culture supernatant to synthesize and secrete DA and NA. After 24 h, samples of the supernatant were collected for use in the DA and NA ELISA tests. The cultured cells were collected and lysed with RIPA buffer (20 mM Tris-HCl (pH 7.4), 150 mM NaCl, 2 mM EDTA, 1% NP-40, 1% deoxycholate, and 0.1% sodium dodecyl sulfate, SDS) containing a complete protease inhibitor cocktail tablet (Roche Diagnostics Ltd., Mannheim, Germany). The amount of protein in the cell lysate was measured using a protein assay BCA kit (FUJIFILM Wako Pure Chemical) according to the manufacturer's protocol. The levels of DA and NA were normalized by the amount of the protein.

In order to assess neurotransmitter levels in various brain regions, the mouse brains were dissected, cut into five parts [prefrontal cortex (Pfc), striatum (Str), hippocampus (Hip), midbrain (Mid), and cerebellum (Cbl)], and frozen in liquid nitrogen. The frozen tissue was suspended in sample buffer (0.01 N HCl, 1 mM EDTA, and 4 mM sodium metabisulfite), and adjusted to 0.1 mg/mL. After homogenization, the tissue suspension was centrifuged and the supernatant was used as the sample for the ELISA. The levels of DA, NA, and 5-HT in each sample were measured using ELISA kits according to the manufacturer's protocol.

2.5. RNA extraction and qPCR

The pCMV6 vector or siRNA was transfected into neuro-2a cells. After 48 h, the cells were collected and dissolved in 0.75 mL of ISOGEN II (Nippon Gene, Tokyo, Japan). Total RNA was extracted from the collected cells according to the manufacturer's protocol. To obtain mRNA from total RNA, 2 μg of extracted total RNA was treated with DNase and then subjected to reverse transcriptase reaction with ReverTra Ace qPCR RT Master Mix with gDNA Remover (TOYOBO, Osaka, Japan) as described in the manufacturer's protocol. Subsequently, mRNA was reacted with a THUNDERBIRD SYBR mix (TOYOBO), as per the manufacturer's instructions, and qPCR analysis was performed using an Applied Biosystems 7300 real-time PCR system (Applied Biosystems, Foster City, CA, USA). PCR primer pairs were selected from different exons of the corresponding genes. The following primers were used for qPCR: forward primer for phenylalanine-4-hydroxylase (*Pah*) (5′-ACTGTCACAGAGTTCCAGCCTC-3′) and reverse primer for *Pah* (5′-TGTCCAGGACCTCAACCCTTTG-3′); forward primer for tyrosine-3-hydroxylase (*Th*) (5′-AAAACCCTCCTCACTGTCTCGG-3′) and reverse primer for *Th* (5′-CGAAGCGCACAAAGTACTCCAG-3′); forward primer for aromatic L-amino acid decarboxylase (*Aadc*) (5′-CAGTTCGCAGAGCTGGACAATC-3′) and reverse primer for *Aadc* (5′-ATCCACCATCTCCTTGCCTCTC-3′); forward primer for dopamine β-hydroxylase (*Dbh*) (5′-GTCTGAGGACTTCCCCCAGTTC-3′) and reverse primer for *Dbh* (5′-GGGAACACCAGCTTCTTTTGGG-3′); forward 2nd primer for *Dbh* (5′-TCGGGATATGCTCAAGGCTCTG-3′) and reverse 2nd primer for *Dbh* (5′-GGTGATCTTAGGCAAAGGCTGC-3′); forward primer for phenylethanolamine *N*-methyltransferase (*Pnmt*) (5′-GCCTATCTCC GCAACAACTACG-3′) and reverse primer for *Pnmt* (5′-GGCCGGAGCCA ATATCAATGAG-3′); forward primer for catechol-*O*-methyltransferase (*Comt*) (5′-TGAGAGAGTCCTACCACAGTGAAAC-3′) and reverse primer for *Comt* (5′-ACAGGAGACCCAATGAGACAGC-3′); forward primer for monoamine oxidase-A (*Mao-A*) (5′-GAAGCCCGGGATAGAGTTG GAG-3′) and reverse primer for *Mao-A* (5′-TGCCTAGCTCCTTAGACAA GCG-3′); forward primer for Solute carrier family 6 member 3 (*Slc6a3*) (5′-CAAAGCTGAAGTCTGACGCTGG-3′) and reverse primer for *Slc6a3* (5′-AGAAGACATTGGTCCCACGGAG-3′); and forward primer for *β-actin* (5′-CCGCGAGCACAGCTTCTTTG-3′) and reverse primer for *β-actin* (5′-GTTGTCGACGACCAGCGCA-3′). For each mRNA, the expression level was normalized using the expression level of *β-actin* mRNA. The relative amount of mRNA in each sample was then calculated by the

comparative ΔCt method [9].

2.6. Western blotting and densitometric quantification

Western blotting was performed as described previously [10]. Briefly, neuro-2a cells were seeded on 12-well tissue culture plates and transfected with mouse *Zfp521* full-length cDNA or a mock vector. Forty-eight hours after transfection, the cells were collected and dissolved in a lysis buffer (0.1 M MES (pH 6.8), 0.5 mM $MgSO_4$, 1 mM EGTA, 2 mM dithiothreitol, and 0.75 M NaCl) containing a complete protease inhibitor cocktail. Next, 10 μg of the sample was electrophoresed on 4–20% gradient SDS polyacrylamide electrophoresis gel (FUJIFILM Wako Pure Chemical), and transferred to an Immobilon-P nylon membrane (Merck Millipore, Bedford, MA, USA). The membrane was incubated in TBS-T buffer (1 × Tris buffer saline, 0.1% Tween 20) containing 5% nonfat dried milk for 1 h and then probed with a primary antibody in TBS-T buffer with milk overnight at 4 °C. Rabbit anti-ZFP521 (ZNF521) polyclonal antibody, rabbit anti-dopamine β-hydroxylase polyclonal antibody, rabbit anti-PHOX2A polyclonal antibody, rabbit anti-EGR-1 monoclonal antibody, rabbit anti-P300 polyclonal antibody and rabbit anti-β-actin polyclonal antibody were used as the primary antibodies. After washing, the membrane was probed with the HRP conjugated anti-rabbit IgG polyclonal antibody for 1 h. The signal was then assessed using an ImmunoStar Zeta Chemiluminescence Detection Kit (FUJIFILM Wako Pure Chemical). The density of each band was quantified using ImageJ software and normalized by the level of β-actin.

2.7. Administration of Nepicastat and behavioral tests

For habituation, a saline solution was administered to mice intraperitoneally daily for two days, and then they were allowed to move freely in the open field for 30 min and on the elevated cross maze for 10 min. On day three, we administered nepicastat to the mice (50 mg/kg weight) as described previously [11]. Behavioral tests were performed from one hour after dosing in the following order: cliff-avoidance test, elevated plus maze, and open field test between 9:00 am and 6:00 pm. Sufficient resting time was allowed between behavioral tests. All mice were identified by an eartag and selected randomly. One or two $Zfp521^{\Delta/\Delta}$ mice and same number of control mice were used for the behavioral tests per day. During experiments and analyses, the investigators were blinded to the genotype and experimental groups. No mice died during the experiments and the data of all mice were used to obtain the results of behavioral tests.

The open field test was performed as described previously [5]. Briefly, an individual mouse was placed on an open field apparatus (60 cm length × 60 cm width) that was divided into a 30 × 30 cm central zone with a surrounding 15 cm wide border zone. The mouse was allowed to freely explore the open field for one hour while the movement of the central point of its body was monitored. The ambulation distance and time spent in the central zone were automatically calculated by EthoVision XT software (Brain Science Idea, Osaka, Japan). After performing the test with each mouse, the arena was cleaned.

The elevated plus maze test was performed as described previously [5]. Briefly, the maze consisted of two open arms (30 × 5 cm, no wall) and two closed arms (30 × 5 cm, surrounded by 15 cm high walls) that emerged from a central platform (5 × 5 cm) and were aligned perpendicularly. All of the mice were individually placed in the central area of the maze and then allowed to move freely for 10 min. The movement of the mice was monitored and the time spent in each arm of the maze was scored by EthoVision XT software. After performing the test with each mouse, the platform was cleaned.

The cliff-avoidance test and jumping events were performed as described previously [5]. The test was initiated by placing an animal on a round platform (an inverted glass cylinder of 20 cm height and 13.5 cm diameter). After performing the tests with each mouse, the arena was cleaned. The time from the initial placement on the platform to falling down was recorded. If the animal remained on the platform after 7 min, then 7 min was used as the jumping time. Cumulative jumping events (%) were calculated as follows: (the number of falling animals/the total number of tested animals) × 100.

2.8. Immunohistochemical analysis and cell count

Five-week-old mice were deeply anesthetized and perfused with 4% paraformaldehyde. The whole brain was removed from the cranium, postfixed for 16 h in 4% PFA in 0.1 M phosphate buffer at pH 7.4, immersed in 30% sucrose in 0.1 M phosphate buffer, washed in 1 × phosphate buffered saline (PBS), dehydrated, and then embedded in paraffin for sectioning. For immunohistochemical staining, 5 μm of paraffin-embedded sections were deparaffinized in xylene, followed by rehydration in a serial dilution of ethanol. Heat-induced antigen retrieval were performed by boiling in 1 × HistoVT One (Nacalai Tesque, Kyoto, Japan) solution for 45 min. Endogenous peroxidase activity was quenched using 0.1% H_2O_2 for 30 min. The slides were washed with 1 × PBS, and then blocked using 2% goat serum albumin (Vector Laboratories, Burlingame, CA, USA) in 1 × PBS. After incubation with rabbit anti-tyrosine hydroxylase polyclonal antibody as the primary antibody, Alexa Fluor 568-conjugated anti-rabbit IgG antibody (Thermo Fisher Scientific) was applied to the tissue sections. After washing with 1 × PBS, nuclei counterstaining was performed with DAPI (Dojindo, Kumamoto, Japan). The slides were mounted with ProLong Diamond Antifade Mountant (Thermo Fisher Scientific), and images were captured using an all-in-one microscope BioRevo BZ-9000 (Keyence, Osaka, Japan). Tyrosine hydroxylase- (TH-) positive cells in the images were counted using dynamic cell count BZ-H1C software (Keyence).

2.9. Statistical analysis

All data are presented as mean ± standard error of the mean (SEM). Statistical analysis was performed using GraphPad Prism 4.0 software (GraphPad Software Inc., San Diego, CA, USA). For the cliff-avoidance test, differences were determined by one-way analysis of variance (ANOVA). For other tests, means were compared by Student's *t*-test. *P*-values < 0.05 were considered statistically significant. Based on previous data [5], we required a minimum of eight animals per group to detect the differences at 95% confidence.

3. Results

3.1. Monoamine levels in brain regions and plasma

Brains of $Zfp521^{\Delta/\Delta}$ and $Zfp521^{+/+}$ mice were divided into Pfc, Str, Hip, Mid, and Cbl and the levels of DA, NA, and 5-HT were measured in each region by ELISA (Fig. 1). DA levels in the Pfc, Str, Hip, and Mid of $Zfp521^{\Delta/\Delta}$ mice were significantly lower than those of $Zfp521^{+/+}$ mice ($P < 0.05$, Fig. 1A). In the Cbl, although it did not reach the level of statistical significance, the DA level of $Zfp521^{\Delta/\Delta}$ mice tended to be lower than that of $Zfp521^{+/+}$ mice ($P = 0.06$). In contrast, NA levels in the Pfc, Str, Hip, Mid, and Cbl of $Zfp521^{\Delta/\Delta}$ mice were significantly higher than those of $Zfp521^{+/+}$ mice ($P < 0.05$, Fig. 1B). For 5-HT levels, no significant differences in any brain regions were observed between the two groups (Fig. 1C). These results suggest that the level of DA is decreased but the level of NA is increased in the brains of $Zfp521^{\Delta/\Delta}$ mice.

We also measured DA and NA levels in plasma (Fig. 1D and E). Consistent with the differences observed in brain monoamines, the level of plasma DA was significantly lower in $Zfp521^{\Delta/\Delta}$ mice than in $Zfp521^{+/+}$ mice, whereas the plasma level of NA was significantly higher in $Zfp521^{\Delta/\Delta}$ mice than in $Zfp521^{+/+}$ mice.

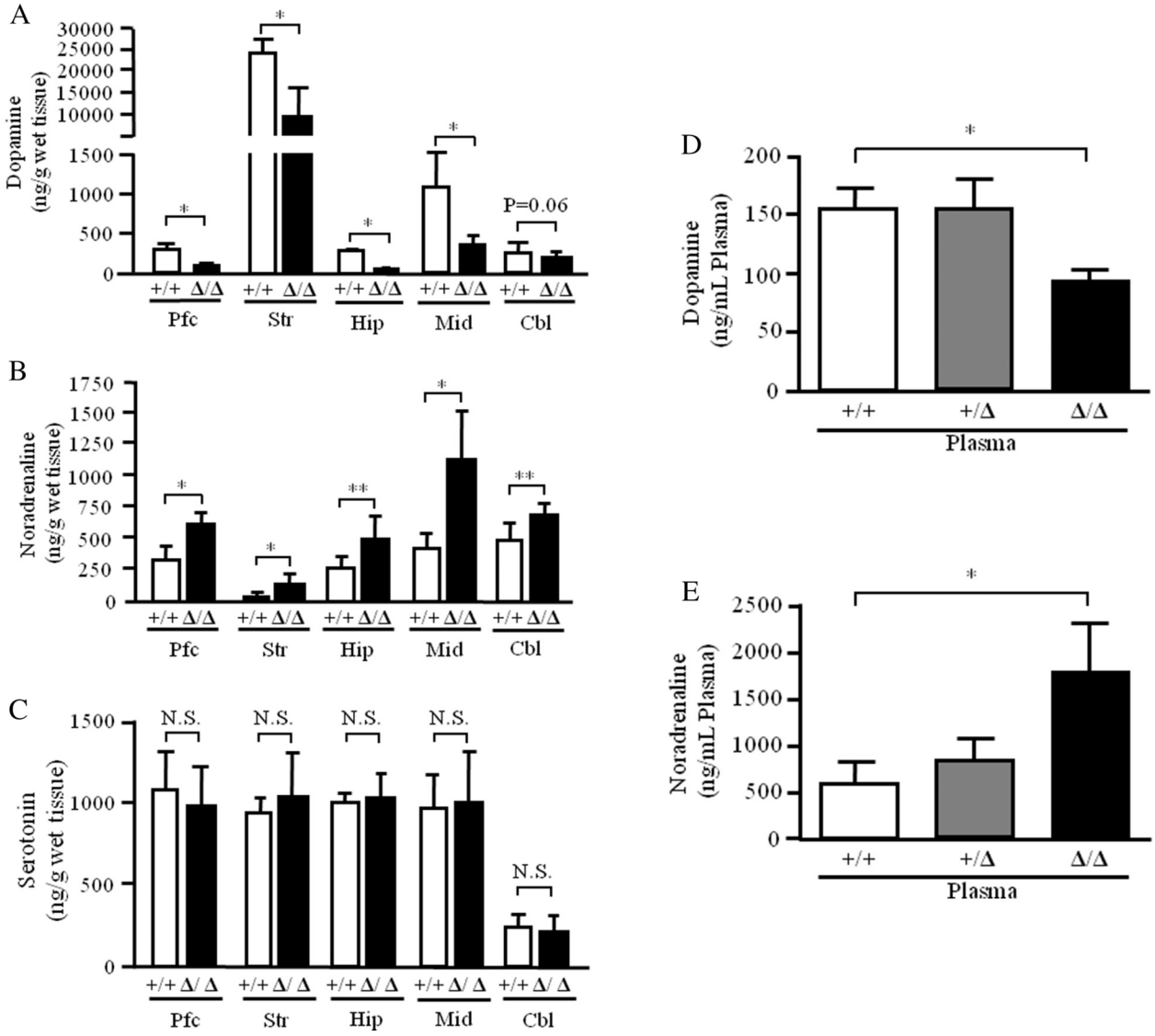

Fig. 1. Measurement of monoamine levels in different brain regions and plasma of *Zfp521*$^{\Delta/\Delta}$ mice. (A–C) Levels of monoamines in the prefrontal cortex (Pfc), striatum (Str), hippocampus (Hip), midbrain (Mid), and cerebellum (Cbl) of mice brains were measured using ELISA. (A) DA level in each region of the brain. Error bars indicate SEM. $N = 8$. $^{*}P < 0.01$, compared to *Zfp521*$^{+/+}$ mice. (B) NA level in each area of the brain. Error bars indicate SEM. $N = 8$. $^{*}P < 0.01$; $^{**}P < 0.05$, compared to *Zfp521*$^{+/+}$ mice. (C) 5-HT level in each area of the brain. Error bars indicate SEM. $N = 8$. NS: no significant difference. (D, E) Levels of DA and NA in the plasma of *Zfp521*$^{\Delta/\Delta}$, *Zfp521*$^{\Delta/+}$, and *Zfp521*$^{+/+}$ mice measured by ELISA. (D) DA levels in the plasma. Error bars indicate SEM. $N = 6$. $^{*}P < 0.01$, compared to *Zfp521*$^{+/+}$ mice. (E) NA levels in the plasma. Error bars indicate SEM. $N = 6$. $^{*}P < 0.01$, compared to *Zfp521*$^{+/+}$ mice.

3.2. DA and NA levels in PC12 cell supernatant

Next, we examined the levels of DA and NA using PC12 cells. In the conditioned medium of PC12 cells transfected with the *Zfp521* expression vector, the level of DA increased and the level of NA decreased (Fig. 2A and B). By contrast, in the conditioned medium of PC12 cells transfected with *Zfp521* siRNA, the level of DA decreased, whereas the level of NA increased (Fig. 2C and D).

3.3. Quantification of mRNA expression levels of catecholamine biosynthetic and metabolic enzymes

In order to clarify why DA decreased and NA increased in the brains of *Zfp521*$^{\Delta/\Delta}$ mice, we quantified mRNA expression levels of five catecholamine biosynthetic enzymes (PAH, TH, AADC, DBH, and PNMT) in whole brains of *Zfp521*$^{\Delta/\Delta}$ mice (Fig. 3A). Of the five catecholamine biosynthetic enzymes examined, only the level of *Dbh* mRNA expression was significantly increased in the brains of *Zfp521*$^{\Delta/\Delta}$ mice ($P < 0.01$). These results were confirmed using another primer set for *Dbh*. *Th* mRNA expression tended to increase in *Zfp521* overexpressing cells compared to control cells, although this difference did not reach the level of statistical significance ($P = 0.07$). There were no differences in the mRNA levels of *Pah*, *Aadc*, or *Pnmt*. We also confirmed the levels of *Comt* and *Mao*, which are metabolic enzymes of catecholamines, but no differences in mRNA levels were observed (Fig. 3B). Similarly, we found no difference in the level of *Slc6a3* mRNA, which is a DA transporter (Fig. 3C). These results may represent the notion that the upregulation of *Dbh* mRNA expression increased the level of DA as its substrate and decreased the level of NA as its product.

3.4. Quantification of protein levels of transcriptional factors of DBH

To determine whether protein levels of DBH, its transcriptional factors, or cofactors correlate with the level of *Dbh* mRNA expression, we transfected the *Zfp521* expression vector into neuro-2a cells and quantified the protein levels of ZFP521, DBH, PHOX2A, EGR-1, P300/

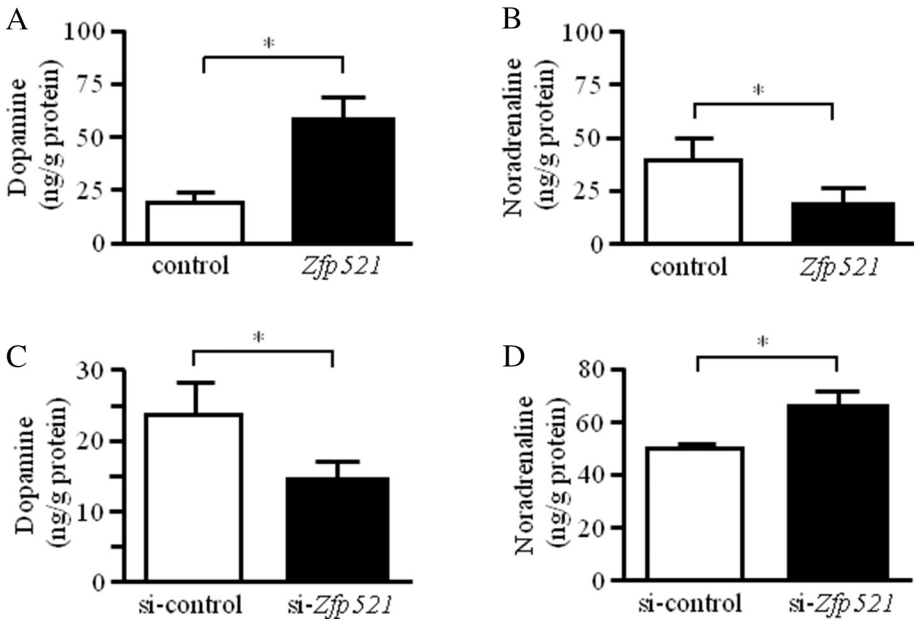

Fig. 2. Measurement of DA and NA levels in the culture supernatant of PC12 cells transfected with *Zfp521* expression vector or siRNA. (A) DA level in the supernatant of *Zfp521* overexpressing PC12 cell culture. The DA level in the supernatant was normalized by the amount of protein from the cells. Data represent mean ± SEM. $N = 8$. $^{*}P < 0.01$, compared to cells transfected with a control vector. (B) NA level in the supernatant of the *Zfp521* overexpressing cell culture. NA level in the supernatant was normalized by the amount of protein from the cells. Data represent mean ± SEM. $N = 8$. $^{*}P < 0.01$ compared to PC12 cells transfected with a control vector. (C) DA level in the supernatant of *Zfp521* siRNA transfected PC12 cells. The DA level in the supernatant was normalized by the amount of protein from the cells. Data represent mean ± SEM. $N = 8$. $^{*}P < 0.01$, compared to PC12 cells transfected with scrambled siRNA. (D) NA level in the supernatant of *Zfp521* siRNA transfected PC12 cells. The NA level in the supernatant was normalized by the amount of protein from the cells. Data represent mean ± SEM. $N = 8$. $^{*}P < 0.01$, compared to PC12 cells transfected with scrambled siRNA.

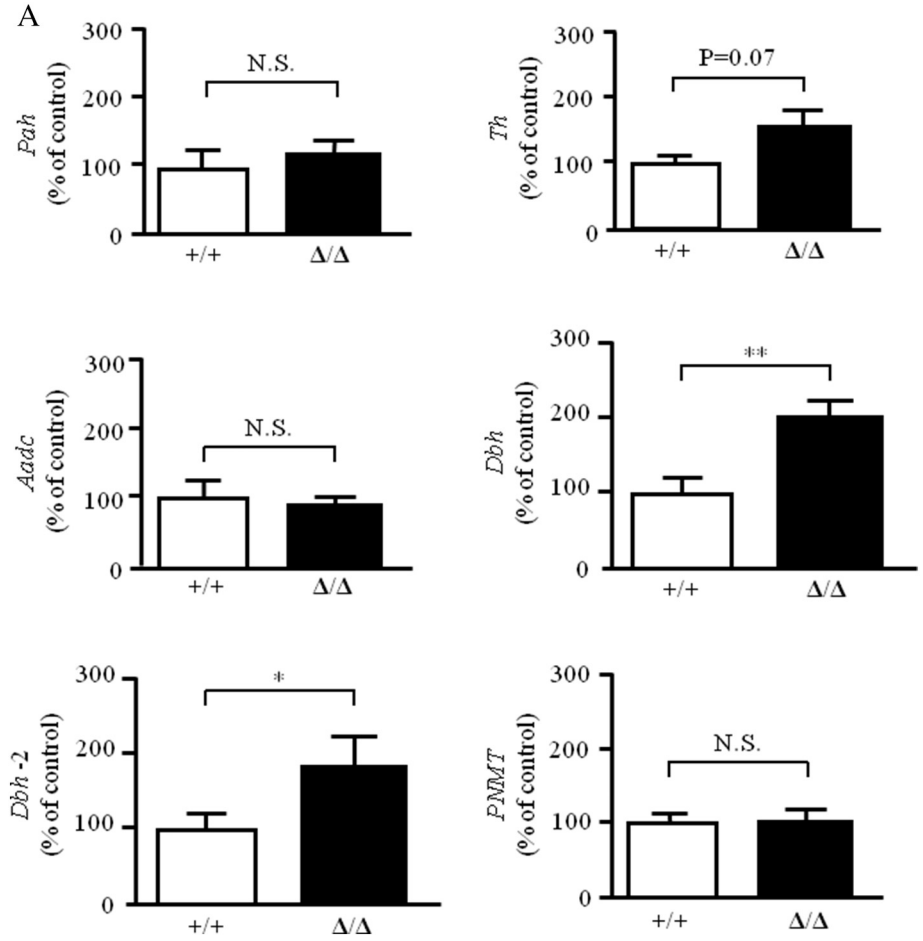

Fig. 3. Analysis of mRNA expression levels of monoamine biosynthetic enzymes. mRNA was extracted from whole brains of $Zfp521^{\Delta/\Delta}$ and $Zfp521^{+/+}$ mice and then subjected to qPCR using primer sets specific for biosynthesis and metabolic enzymes. (A) The mRNA expression levels of phenylalanine-4-hydroxylase (*Pah*), tyrosine hydroxylase (*Th*), aromatic L-amino acid decarboxylase (*Aadc*), dopamine β-hydroxylase (*Dbh*), and phenylethanolamine *N*-methyltransferase (*Pnmt*). The *Dbh*-2 graph shows the expression of *Dbh* mRNA using another primer set. The expression level of each enzyme was normalized by the level of *β-actin*. Data represent mean ± SEM. $N = 7$. NS: no significant difference. $^{*}P < 0.01$, $^{**}P < 0.05$. compared to $Zfp521^{+/+}$ mice. (B) The mRNA expression levels of catechol-*O*-methyltransferase (*Comt*) and monoamine oxidase-A (*Mao-a*). The expression level of each enzyme was normalized by the level of *β-actin*. Data represent mean ± SEM. $N = 7$. NS: no significant difference. $^{**}P < 0.05$, compared to $Zfp521^{+/+}$ mice. (C) The mRNA expression levels of sodium-dependent DA transporter (*Slc6a3*). Data represent mean ± SEM. $N = 7$. NS: no significant difference compared to $Zfp521^{+/+}$ mice.

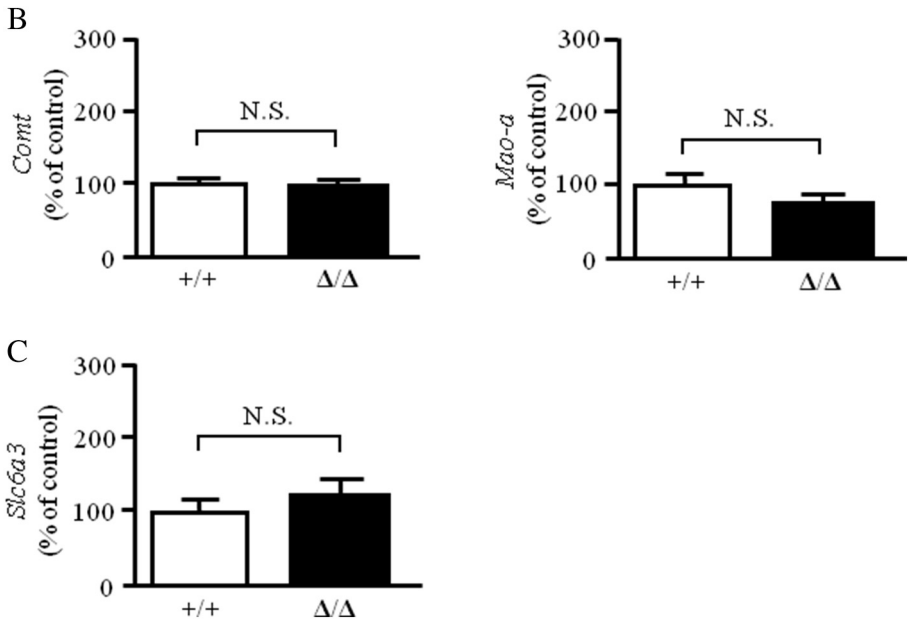

Fig. 3. (*continued*)

CBP, and β-actin in *Zfp521* expressing cells by western blot and densitometric quantification (Fig. 4A and B). The expression level of β-actin was used as a loading standard. Abundant expression of *Zfp521* protein was ascertained in cells transfected with *Zfp521* expression vector by western blotting. We also confirmed that the level of DBH expression decreased in accordance with the level of ZFP521 protein upregulation. PHOX2 and EGR-1, which are the major transcriptional factors of *Dbh*, and their binding to the *cis*-acting element on the *Dbh* promoter enhanced the expression of the DBH protein. We thus examined the levels of PHOX2A and EGR-1 protein expression and found that both were significantly decreased in *Zfp521* expressing cells. The scaffold protein P300/CBP is known to form a complex with transcriptional factors including PHOX2A and EGR-1. P300/CBP can form a complex with ZFP521 via the early B-cell factor (EBF) family protein. Therefore, we examined the level of P300/CBP protein by western blotting. However, the levels did not differ between *Zfp521* expressing cells and control cells.

3.5. Quantification of mRNA levels of transcriptional factors of DBH

Having demonstrated that the amount of proteins of DBH and its transcription factors decreased in *Zfp521* expressing neuro-2a cells, we then transfected the *Zfp521* expression vector into neuro-2a cells and quantified the mRNA levels of *Dbh* and its transcriptional factors in these cells by qPCR (Fig. 4C). First, we confirmed the upregulation of *Zfp521* mRNA levels. The mRNA levels of *Phox2a* and *Egr-1* were significantly suppressed by *Zfp521* expression. This study shows that the overexpression of *Zfp521* suppresses the transcription of the DBH transcription factors *Phox2a* and *Egr-1*. Next, we investigated whether mRNA expression levels of *Phox2a* and *Egr-1* were upregulated by *Zfp521* knockdown by siRNA (Fig. 4D). qPCR using neuro-2a cells transfected with *Zfp521* siRNA confirmed that mRNA levels of *Phox2a* and *Egr-1* were increased.

3.6. Behavioral tests of mice given Nepicastat

Our previous report revealed that *Zfp521*$^{\Delta/\Delta}$ mice exhibited abnormal behaviors, including higher locomotor activity and lower anxiety level, compared to *Zfp521*$^{+/+}$ mice. In order to determine whether these abnormal behaviors were due to alteration of DBH expression, behavioral tests were performed after administration of the DBH inhibitor nepicastat. To confirm the effect of nepicastat on DBH in mice, plasma DA and NA were measured 6 h after administration. After administration of nepicastat, the levels of DA increased and NA decreased in the plasma of both *Zfp521*$^{\Delta/\Delta}$ and *Zfp521*$^{+/+}$ mice (Fig. 5A and B).

We then performed open field tests to examine the locomotor activity and anxiety. In *Zfp521*$^{+/+}$ mice, the administration of nepicastat did not change the total ambulation distance and spent time in the central area (Figs. 5C–E). However, in *Zfp521*$^{\Delta/\Delta}$ mice, nepicastat administration reduced the total ambulation distance and the spent time in the central area. Taken together, these results indicate that nepicastat administration reduced the levels of anxiety and locomotion in *Zfp521*$^{\Delta/\Delta}$ mice.

We also performed the elevated plus maze test to confirm that nepicastat reduces anxiety levels (Figs. 5F–5H). For *Zfp521*$^{\Delta/\Delta}$ mice, the administration of nepicastat decreased the total distance of ambulation (Fig. 5F and G). By contrast, nepicastat had no effect on the decreased total distance of ambulation for *Zfp521*$^{+/+}$ mice. Next, we measured the amount of time spent in each arm of the maze and the central zone during a 10 min observation period (Fig. 5H). After the administration of nepicastat, *Zfp521*$^{\Delta/\Delta}$ mice spent less time in the open arms and more time in closed arms and the central zone. By contrast, nepicastat had no effect on the time spent in each location for *Zfp521*$^{+/+}$ mice. These results indicate that the levels of anxiety and locomotion in *Zfp521*$^{\Delta/\Delta}$ mice are decreased by nepicastat.

Lastly, we performed the cliff-avoidance test to assess the maladaptive impulsive behavior (Fig. 5I). In contrast to the 85% of *Zfp521*$^{+/+}$ mice that remained on the platform after 7 min, all of the *Zfp521*$^{\Delta/\Delta}$ mice demonstrated to fall down from the platform within 6 min. After the administration of nepicastat, 25% of the *Zfp521*$^{\Delta/\Delta}$ mice remained on the platform after 7 min.

3.7. Cell count in the locus Coeruleus (LC)

It is widely known that most NA released in the brain is supplied from the LC. We considered the possibility that the elevated NA levels observed in *Zfp521*$^{\Delta/\Delta}$ mice were caused by an increase in the number of cells in the LC. In order to assess this hypothesis, we performed an immunohistochemical analysis using an anti-TH antibody specific for NAergic LC cells and then counted the TH-positive cells (Fig. 6A and B). The number of TH-positive cells in the LC was smaller in *Zfp521*$^{\Delta/\Delta}$

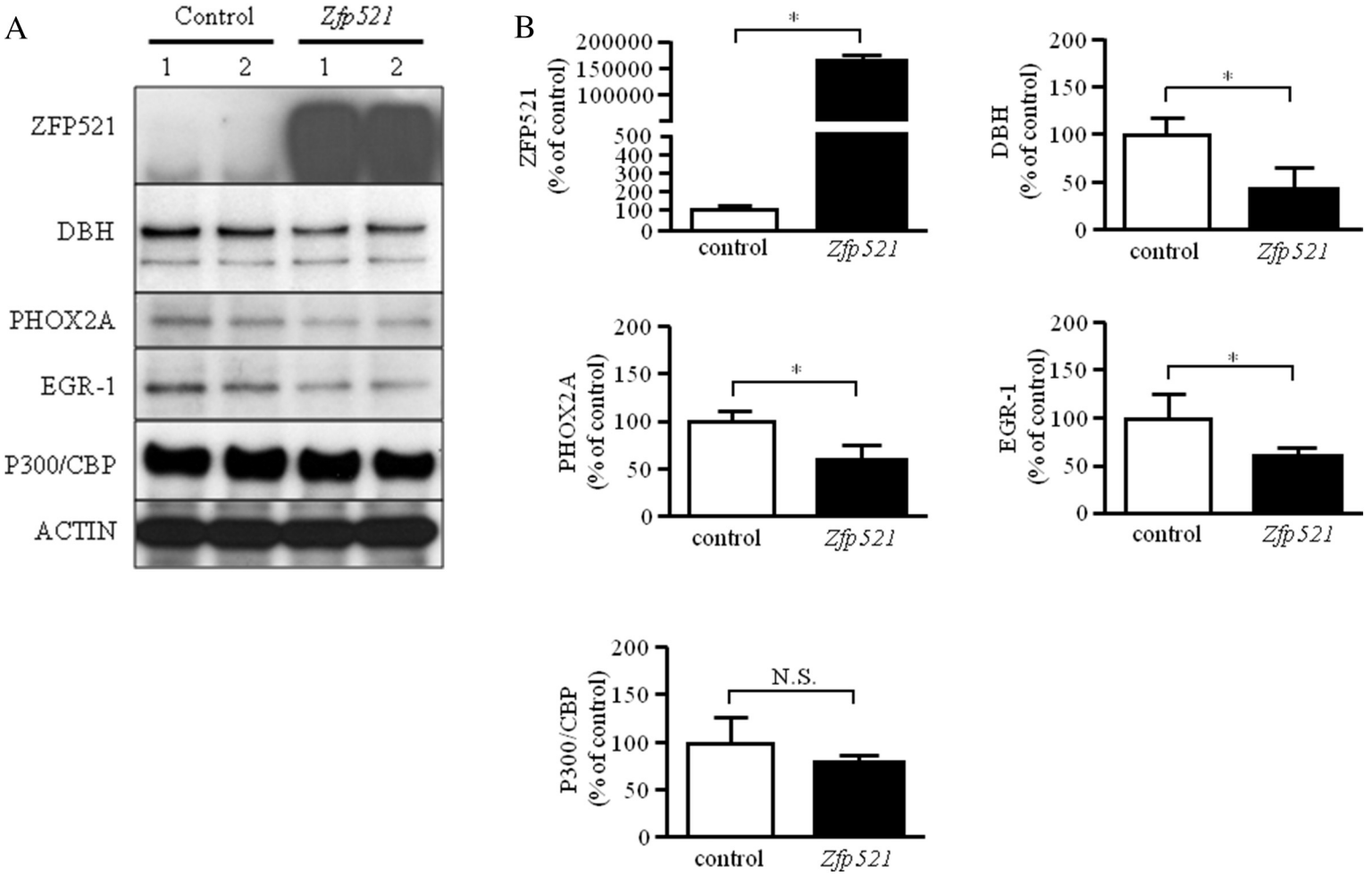

Fig. 4. Analysis of protein and mRNA expression levels of DBH transcriptional factors in neuro-2a cells transfected with the *Zfp521* expression vector or siRNA. (A) Western blotting results. Western blots of lysates from *Zfp521*-overexpressing cells were probed with anti-ZFP521, anti-DBH, anti-PHOX2A, anti-EGR-1, and anti-P300 antibodies. Anti-*β-actin* antibody (bottom panel) was used as a control for protein loading. $N = 6$. (B) Densitometric quantification of ZFP521, DBH, PHOX2A, EGR-1, and P300 protein in *Zfp521* overexpressing cells. The density of each band shown above was quantified using ImageJ software and normalized by *β-actin*. Data represent mean ± SEM. $N = 6$. $^{*}P < 0.01$, compared to cells transfected with the control vector. (C) Measurement of mRNA expression levels of *Dbh* and its transcription factors in *Zfp521* overexpressing cells. mRNA was extracted from *Zfp521*-overexpressing cells and subjected to qPCR using the primer sets for *Zfp521*, *Dbh*, *Phox2a*, and *Egr-1*. The expression level of each enzyme was normalized by the level of *β-actin*. Data represent mean ± SEM. $N = 8$. $^{*}P < 0.01$, compared to control vector transfected neuro-2a cells. (D) Measurement of mRNA expression levels of *Dbh* and its transcription factors in neuro-2a cells transfected with *Zfp521* siRNA. mRNA was extracted from neuro-2a cells transfected with *Zfp521* siRNA and subjected to qPCR using the primer sets for *Zfp521*, *Phox2a*, and *Egr-1*. The expression level of each enzyme was normalized by the level of *β-actin*. Data represent mean ± SEM. $N = 8$. $^{*}P < 0.01$, compared to neuro-2a cells transfected with scrambled siRNA.

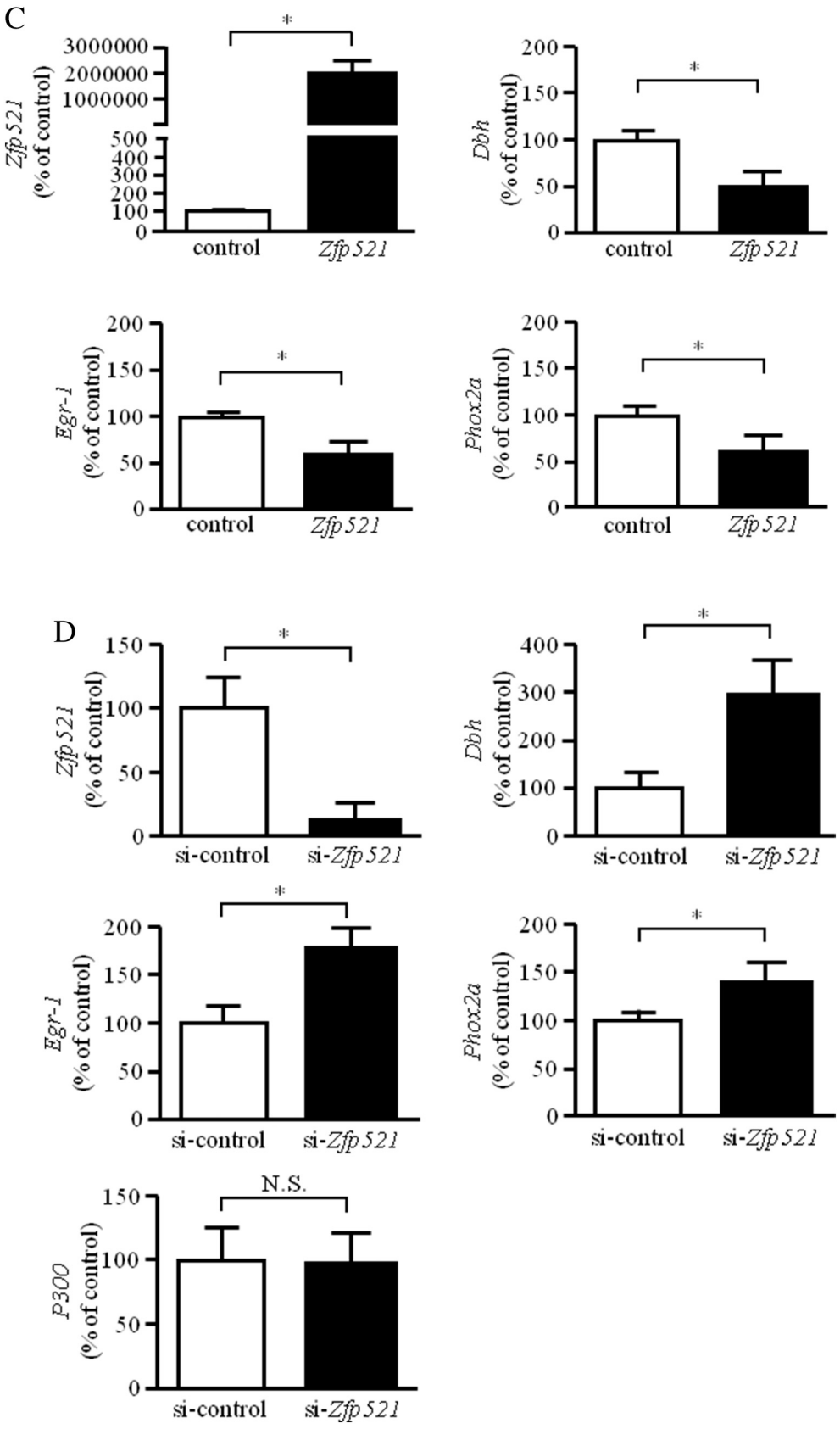

Fig. 4. (*continued*)

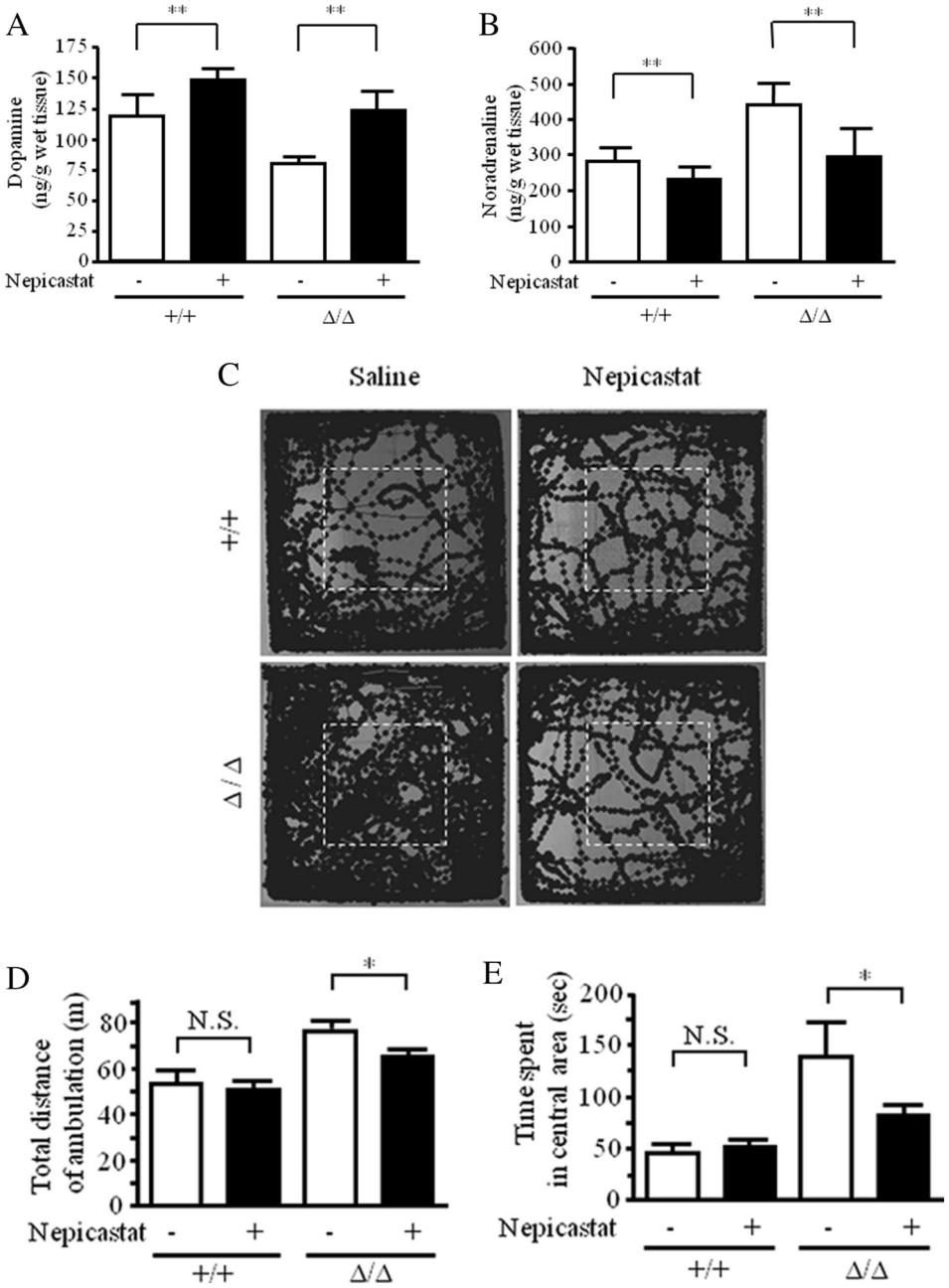

Fig. 5. Behavioral analysis. (A) DA level in whole brains of *Zfp521*$^{+/+}$ and *Zfp521*$^{\Delta/\Delta}$ mice treated or untreated with nepicastat. Data represent mean ± SEM. $N = 8–10$. $^{**}P < 0.05$. (B) NA levels in the whole brains of *Zfp521*$^{+/+}$ and *Zfp521*$^{\Delta/\Delta}$ mice treated or untreated with nepicastat. Data represent mean ± SEM. $N = 8–10$. $^{*}P < 0.01$; $^{**}P < 0.05$. (C–E) Open field test. (C) Representative locomotor tracks of *Zfp521*$^{\Delta/\Delta}$ (lower panels) and *Zfp521*$^{+/+}$ mice (upper panels) treatment (right panels) or untreated (left panels) with nepicastat during a period of 60 min. The white dashed box in the open field is the central area. (D) Total distance of ambulation of *Zfp521*$^{\Delta/\Delta}$ and *Zfp521*$^{+/+}$ mice treated or untreated with nepicastat during a period of 60 min. Data represent mean ± SEM. $N = 8–10$. $^{*}P < 0.01$. (E) Time spent in the central area. *Zfp521*$^{\Delta/\Delta}$ mice treated with nepicastat spent less time in the central area of the open field than *Zfp521*$^{\Delta/\Delta}$ mice untreated with nepicastat. Data represent mean ± SEM. $N = 8–10$. $^{*}P < 0.01$. (F—H) Elevated plus maze test. (F) Representative locomotor tracks of *Zfp521*$^{\Delta/\Delta}$ mice (lower panels) and *Zfp521*$^{+/+}$ mice (upper panels) treated (right panels) or untreated (left panels) with nepicastat during a period of 10 min. C: closed arm; O: open arm. (G) Total distance of ambulation of *Zfp521*$^{\Delta/\Delta}$ and *ZFP521*$^{+/+}$ mice treated or untreated with nepicastat. Data represent mean ± SEM. $N = 8–10$. $^{*}P < 0.01$; $^{**}P < 0.05$. (H) Time spent in closed arms, open arms, and central area. Data represent mean ± SEM. $N = 8–10$. $^{*}P < 0.01$; $^{**}P < 0.05$. NS: no significant difference. (I) Cliff-avoidance test. ●: *Zfp521*$^{+/+}$ mice untreated with nepicastat; ○: *Zfp521*$^{+/+}$ mice treated with nepicastat; ▲: *Zfp521*$^{\Delta/\Delta}$ mice untreated with nepicastat; △: *Zfp521*$^{\Delta/\Delta}$ mice untreated with nepicastat. The cumulative frequency of jumping was determined. $N = 16–20$. $^{*}P < 0.01$.

mice than in *Zfp521*$^{+/+}$ mice. This suggests that the elevated NA levels seen in *Zfp521*$^{\Delta/\Delta}$ mice are not due to an increased number of cells in the LC.

4. Discussion

The locomotor behavior in mice is reported to be dependent on the quantitative balance between DA and NA [12]. In children affected by attention deficit hyperactivity disorder (ADHD), altered DA due to dysfunction of Pfc has been reported [13]. Drugs that regulate NA

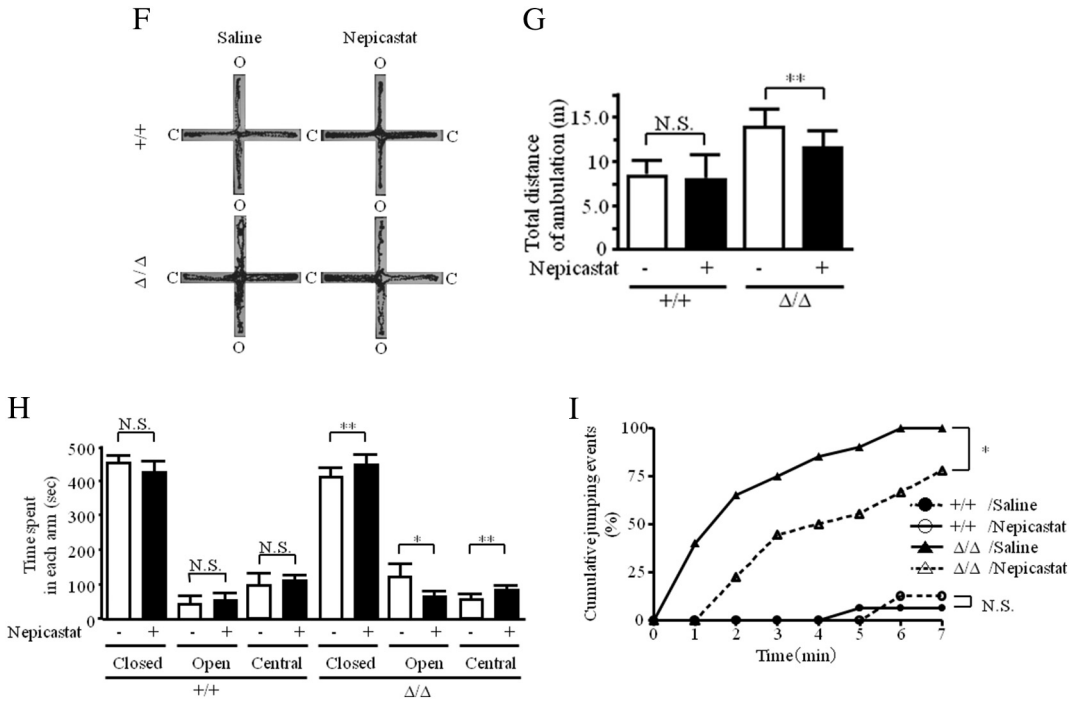

Fig. 5. (*continued*)

transmission, such as methylphenidate and amphetamine, are effective for patients with ADHD [14,15] and return the quantitative DA and NA balance closer to the normal state [16–18]. Given these findings, we suggest that DA/NA imbalance due to decreased DA and increased NA in the brain causes the abnormal behavior of *Zfp521*$^{\Delta/\Delta}$ mice, including hyperlocomotion and reduced anxiety.

We demonstrated decreased DA and increased NA levels in most parts of the brains of *Zfp521*$^{\Delta/\Delta}$ mice, compared to *Zfp521*$^{+/+}$ mice (Fig. 1A and B). These results suggested that the intracellular synthesis or metabolism of these neurotransmitters is altered. This finding is consistent with that of lower DA and higher NA levels in the supernatant of PC12 cells transfected with *Zfp521* siRNA relative to scrambled siRNA (Fig. 2C and D). We also demonstrated that the mRNA level of *Slc6a3*, a DA transporter, was not significantly altered (Fig. 3C), suggesting that intracranial transport of DA and NA is not impaired in *Zfp521*$^{\Delta/\Delta}$ mice.

We demonstrated that the mRNA level of *Dbh*, the enzyme that converts DA into NA, was elevated in the brains of *Zfp521*$^{\Delta/\Delta}$ mice (Fig. 3A). This result is consistent with the increased mRNA level of *Dbh* in neuro-2a cells transfected with *Zfp521* siRNA relative to scrambled siRNA (Fig. 4D). Complete deficiency of NA has been reported in *Dbh*-deficient mice with elevated DA levels in most tissues [19]. *Dbh*-deficient mice also exhibited abnormal behaviors, including slow swimming [20].

The transcriptional regulatory system of the *Dbh* gene has been investigated in detail, and its main factor is the homeodomain box transcription factor PHOX2 [21]. *Phox2a*-deficient mice show deficiency of DBH expression and absence of LC [22]. PHOX2 binds to the homeodomain box binding site in the promoter of the *Dbh* gene to promote the transcription of DBH [23]. The transcription factor EGR-1 also binds to the *Dbh* promoter [24]. In this study, overexpression and underexpression of *Zfp521*, respectively, negatively and positively regulated mRNA levels of *Dbh*, *Phox2a*, and *Egr-1* in neuro-2a neuronal cells (Fig. 4C and D). From these results, we deduce that *Zfp521* suppressed the expression of PHOX2 and EGR-1, and their reduction negatively regulated the expression of DBH.

PHOX2A and EGR-1 form complicated complexes with the coactivator P300/CBP, and other transcription factors, such as specificity protein 1 (SP1), cAMP response element binding protein (CREB), and this complex bind to HD sites of the *Dbh* promoter, thereby regulating its expression [25]. The ZFP521 protein binds to P300 via EBF family proteins [26]. Therefore, we deduce that ZFP521 may regulate the expression of P300 and the functions of PHOX2A and EGR-1. However, as shown by the western blotting results, the expression levels of P300/CBP protein did not change with the overexpression of ZFP521 (Fig. 4A and B). Furthermore, acetylation of P300 did not change with the overexpression of ZFP521 (data not shown). Thus, changes in the expression levels of PHOX2A and EGR-1 by ZFP521 do not appear to be mediated by P300.

ZFP521 is known to regulate stem cell differentiation in various tissues [27,28]. For example, ZFP521 plays a role in cell fate switching critical for bone morphogenetic protein (BMP)-induced osteoblast commitment and repressed adipocyte commitment [29,30]. In the nervous system, ZFP521 is a factor that promotes differentiation from epiblasts into neuroectodermal cells [31]. The transcription factor PHOX2, which was shown to be negatively regulated by ZFP521 in this study, plays a role in the differentiation of neural crest cells into catecholaminergic neurons [32]. Therefore, we examined whether the number of cells in the LC, the main nucleus of NAergic cells, was increased in *Zfp521*$^{\Delta/\Delta}$ mice. However, contrary to this expectation, the number of cells was reduced (Fig. 6A and B). This finding suggests that changes in catecholamine and DBH expression levels in *Zfp521*$^{\Delta/\Delta}$ mice are not attributable to changes in cell numbers due to abnormal differentiation of NAergic cells in the LC.

Nepicastat is an antagonist that binds to the active site of DBH. It has high selectivity to DBH and few side effects and can reach the brain parenchyma through the blood–brain barrier [33]. We measured the expression level of *Dbh* mRNA by qPCR using mRNA extracted from whole brains of *Zfp521*$^{\Delta/\Delta}$ mice intraperitoneally injected with nepicastat. The expression level of *Dbh* mRNA was increased in the brain (data not shown), which may be due to a compensatory mechanism that increases the expression of *Dbh* mRNA when DBH activity is attenuated. Increased DA and decreased NA levels were observed in the brains of *Zfp521*$^{\Delta/\Delta}$ mice (Fig. 5A and B), confirming that DBH function was successfully suppressed by the administration of nepicastat. This result is consistent with a report of increased DA and decreased NA in the

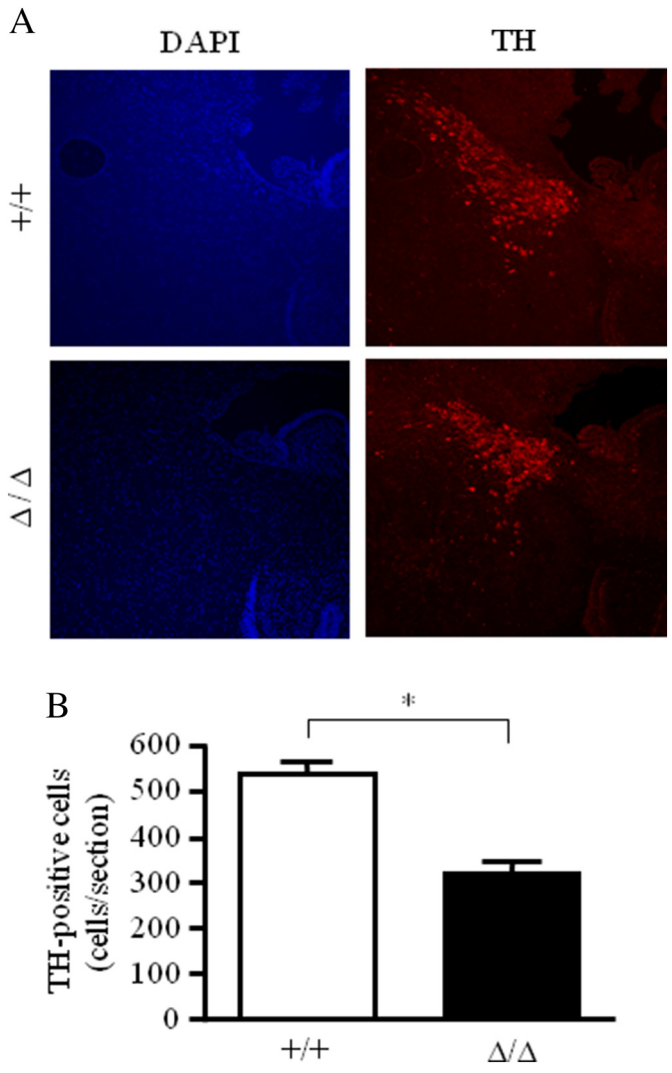

Fig. 6. Histological analysis of LC. (A) Immunohistochemical detection of TH-positive LC cells. Sagittal sections from *Zfp521*$^{\Delta/\Delta}$ (lower panel) and *Zfp521*$^{+/+}$ mice (upper panel) were stained with anti-TH antibodies. Bars = 100 μm. (B) Quantification of the number of cells in the LC. Data represent mean ± SEM. $N = 6$. $^{*}P < 0.01$.

supernatant of nepicastat-administered PC12 cells [33]. It is also consistent with a report that nepicastat reduced NA in the Pfc and nucleus accumbens but increased DA in the medial Pfc [34]. In our previous paper, we reported that the abnormal behaviors seen in *Zfp521*$^{\Delta/\Delta}$ mice were similar to the symptoms of schizophrenia [5]. Several studies support the notion that the brain DA-NA system may play a role in the onset of schizophrenia [35,36]. For example, elevated NA levels in the cerebrospinal fluid and plasma have been reported in patients with schizophrenia [37]. Yamamoto et al. reported that DBH might be a modulator of psychotic symptoms, severity of the disorder, and therapeutic response to neuroleptic drugs [38]. In this study, nepicastat inhibited the aberrant behaviors of *Zfp521*$^{\Delta/\Delta}$ mice through the suppression of DBH. Therefore, we deduce that these abnormal behaviors were caused by decreased DA and increased NA in the brain due to the upregulation of DBH.

5. Conclusion

Using *Zfp521*$^{\Delta/\Delta}$ mice and *Zfp521*-transfected cells, we demonstrated that ZFP521 regulates DA and NA levels by negatively regulating the level of DBH. We also revealed that the regulation of the DBH transcription factor at the mRNA level is involved in this mechanism. Furthermore, the findings suggest that DBH elevation is involved in the abnormal behaviors observed in *Zfp521*$^{\Delta/\Delta}$ mice.

Author contributions

Nobutaka Ohkubo: Conceptualization, Methodology, Formal Analysis, Data Curation, Writing- Original Draft, Visualization, Project administration. **Mamoru Aoto:** Writing-Reviewing and Editing. **Kazunori Kon:** Validation, Investigation, Resources. **Noriaki Mitsuda:** Writing-Reviewing and Editing, Supervision.

Funding sources

This research did not receive any specific grant from funding agencies in the public, commercial, or not-for-profit sectors.

Acknowledgements

This work was supported by the Department of Bioscience and the Department of Biological Resources, ADRES, Ehime University. The authors would like to thank Enago (www.enago.jp) for the English language review.

Declaration of Competing Interest

The authors declare that there are no conflicts of interests.

References

[1] E. Hesse, R. Kiviranta, M. Wu, H. Saito, K. Yamana, D. Correa, A. Atfi, D. Baron, Zinc finger protein 521, a new player in bone formation, Ann. N. Y. Acad. Sci. 1192 (2010) 32–37, https://doi.org/10.1111/j.1749-6632.2009.05347.x.
[2] S. Warming, P. Liu, T. Suzuki, K. Akagi, S. Lindtner, G.N. Pavlakis, N.A. Jenkins, N.G. Copeland, Evi3, a common retroviral integration site in murine B-cell lymphoma, encodes an EBFAZ-related Krüppel-like zinc finger protein, Blood 101 (2003) 1934–1940.
[3] D. Kamiya, S. Banno, N. Sasai, M. Ohgushi, H. Inomata, K. Watanabe, M. Kawada, R. Yakura, H. Kiyonari, K. Nakao, L.M. Jakt, S. Nishikawa, Y. Sasai, Intrinsic transition of embryonic stem-cell differentiation into neural progenitors, Nature 470 (2011) 503–509, https://doi.org/10.1038/nature09726.
[4] M.K. Lobo, C. Yeh, X.W. Yang, Pivotal role of early B-cell factor 1 in development of striatonigral medium spiny neurons in the matrix compartment, J. Neurosci. Res. 86 (2008) 2134–2146, https://doi.org/10.1002/jnr.21666.
[5] N. Ohkubo, E. Matsubara, J. Yamanouchi, R. Akazawa, M. Aoto, Y. Suzuki, I. Sakai, T. Abe, H. Kiyonari, S. Matsuda, M. Yasukawa, N. Mitsuda, Abnormal behaviors and developmental disorder of hippocampus in zinc finger protein (ZFP521) mutant mice, PLoS One 9 (2014) e92848, , https://doi.org/10.1371/journal.pone.0092848.
[6] R. Moraga-Amaro, H. Gonzalez, R. Pacheco, J. Stehberg, Dopamine receptor D3 deficiency results in chronic depression and anxiety, Behav. Brain Res. 274 (2014) 186–193, https://doi.org/10.1016/j.bbr.2014.07.055.
[7] R.D. Oades, K. Taghzouti, J.M. Rivet, H. Simon, M. Le Moal, Locomotor activity in relation to dopamine and noradrenaline in nucleus accumbens, septal and frontal areas: a 6-hydroxydopamine study, Neuropsychobiology 16 (1986) 37–42.
[8] M.D. Jones, E.J. Hess, Norepinephrine regulates locomotor hyperactivity in the mouse mutant coloboma, Pharmacol. Biochem. Behav. 75 (2003) 209–219.
[9] T.D. Schmittgen, K.J. Livak, Analyzing real-time PCR data by the comparative C(T) method, Nat. Protoc. 3 (2008) 1101–1108.
[10] N. Ohkubo, Y.D. Lee, A. Morishima, T. Terashima, S. Kikkawa, M. Tohyama, M. Sakanaka, J. Tanaka, N. Maeda, M.P. Vitek, N. Mitsuda, Apolipoprotein E and Reelin ligands modulate tau phosphorylation through an apolipoprotein E receptor/disabled-1/glycogen synthase kinase-3β cascade, FASEB J. 17 (2003) 295–297.
[11] M. Gaval-Cruz, L.C. Liles, P.M. Iuvone, D. Weinshenker, Chronic inhibition of dopamine β-hydroxylase facilitates behavioral responses to cocaine in mice, PLoS One 7 (2012) e50583, , https://doi.org/10.1371/journal.pone.0050583.
[12] D. Viggiano, L.A. Ruocco, S. Arcieri, A.G. Sadile, Involvement of norepinephrine in the control of activity and attentive processes in animal models of attention deficit hyperactivity disorder, Neural Plast. 11 (2004) 133–149.
[13] E. Jodo, C. Chiang, G. Aston-Jones, Potent excitatory influence of prefrontal cortex activity on noradrenergic locus coeruleus neurons, Neuroscience 83 (1998) 63–79.
[14] M.V. Solanto, Dopamine dysfunction in AD/HD: integrating clinical and basic neuroscience research, Behav. Brain Res. 130 (2002) 65–71.
[15] A.F. Arnsten, Stimulants: therapeutic action in ADHD, Neuropsychopharmacology 31 (2006) 2376–2383.
[16] D. Lacroix, A. Ferron, Electrophysiological effects of methylphenidate on the

coeruleo-cortical noradrenergic system in the rat, Eur. J. Pharmacol. 149 (1988) 277–285.
[17] N. Easton, C. Steward, F. Marshall, K. Fone, C. Marsden, Effects of amphetamine isomers, methylphenidate and atomoxetine on synaptosomal and synaptic vesicle accumulation and release of dopamine and noradrenaline in vitro in the rat brain, Neuropharmacology 52 (2007) 405–414.
[18] R. Kuczenski, D.S. Segal, Locomotor effects of acute and repeated threshold doses of amphetamine and methylphenidate: relative roles of dopamine and norepinephrine, J. Pharmacol. Exp. Ther. 296 (2001) 876–883.
[19] S.A. Thomas, R.D. Palmiter, Impaired maternal behavior in mice lacking norepinephrine and epinephrine, Cell 91 (1997) 583–592.
[20] S.A. Thomas, B.T. Marck, R.D. Palmiter, A.M. Matsumoto, Restoration of norepinephrine and reversal of phenotypes in mice lacking dopamine beta-hydroxylase, J. Neurochem. 70 (1998) 2468–2476.
[21] H. Seo, S.J. Hong, S. Guo, H.S. Kim, C.H. Kim, D.Y. Hwang, O. Isacson, A. Rosenthal, K.S. Kim, A direct role of the homeodomain proteins Phox2a/2b in noradrenaline neurotransmitter identity determination, J. Neurochem. 80 (2002) 905–916.
[22] X. Morin, H. Cremer, M.R. Hirsch, R.P. Kapur, C. Goridis, J.F. Brunet, Defects in sensory and autonomic ganglia and absence of locus coeruleus in mice deficient for the homeobox gene Phox2a, Neuron 18 (1997) 411–423.
[23] H.S. Kim, H. Seo, C. Yang, J.F. Brunet, K.S. Kim, Noradrenergic-specific transcription of the dopamine beta-hydroxylase gene requires synergy of multiple cis-acting elements including at least two Phox2a-binding sites, J. Neurosci. 18 (1998) 8247–8260.
[24] S.Y. Cheng, L.I. Serova, D. Glazkova, E.L. Sabban, Regulation of rat dopamine beta-hydroxylase gene transcription by early growth response gene 1, Brain Res. 1193 (2008) 1–11, https://doi.org/10.1016/j.brainres.2007.11.055.
[25] D.J. Swanson, M. Adachi, E.J. Lewis, The homeodomain protein Arix promotes protein kinase A-dependent activation of the dopamine beta-hydroxylase promoter through multiple elements and interaction with the coactivator cAMP-response element-binding protein-binding protein, J. Biol. Chem. 275 (2000) 2911–2923.
[26] D. Liao, Emerging roles of the EBF family of transcription factors in tumor suppression, Mol. Cancer Res. 7 (2009) 1893–1901, https://doi.org/10.1158/1541-7786.MCR-09-0229.
[27] B.S. Garrison, A.P. Rybak, I. Beerman, B. Heesters, F.E. Mercier, D.T. Scadden, D. Bryder, R. Baron, D.J. Rossi, ZFP521 regulates murine hematopoietic stem cell function and facilitates MLL-AF9 leukemogenesis in mouse and human cells, Blood 130 (2017) 619–624, https://doi.org/10.1182/blood-2016-09-738591.
[28] T. Hiratsuka, Y. Takei, R. Ohmori, Y. Imai, M. Ozeki, K. Tamaki, H. Haga, T. Nakamura, T. Tsuruyama, ZFP521 contributes to pre-B-cell lymphoma genesis through modulation of the pre-B-cell receptor signaling pathway, Oncogene 35 (2016) 3227–3238, https://doi.org/10.1038/onc.2015.385.
[29] S. Kang, P. Akerblad, R. Kiviranta, R.K. Gupta, S. Kajimura, M.J. Griffin, J. Min, R. Baron, E.D. Rosen, Regulation of early adipose commitment by Zfp521, PLoS Biol. 10 (2012) e1001433, , https://doi.org/10.1371/journal.pbio.1001433.
[30] W.N. Addison, M.M. Fu, H.X. Yang, Z. Lin, K. Nagano, F. Gori, R. Baron, Direct transcriptional repression of Zfp423 by Zfp521 mediates a bone morphogenic protein-dependent osteoblast versus adipocyte lineage commitment switch, Mol. Cell. Biol. 34 (2014) 3076–3085, https://doi.org/10.1128/MCB.00185-14.
[31] S. Shen, J. Pu, B. Lang, C.D. McCaig, A zinc finger protein Zfp521 directs neural differentiation and beyond, Stem Cell Res Ther 2 (2011) 20–24, https://doi.org/10.1186/scrt61.
[32] A. Pattyn, X. Morin, H. Cremer, C. Goridis, J.F. Brunet, The homeobox gene Phox2b is essential for the development of autonomic neural crest derivatives, Nature 399 (1999) 366–370.
[33] W.C. Stanley, B. Li, D.W. Bonhaus, L.G. Johnson, K. Lee, S. Porter, K. Walker, G. Martinez, R.M. Eglen, R.L. Whiting, S.S. Hedge, Catecholamine modulatory effects of nepicastat (RS-25560-197), a novel, potent and selective inhibitor of dopamine-beta-hydroxylase, Br. J. Pharmacol. 121 (1997) 1803–1809.
[34] P. Devoto, G. Flore, P. Saba, V. Bini, G.L. Gessa, The dopamine beta-hydroxylase inhibitor nepicastat increases dopamine release and potentiates psychostimulant-induced dopamine release in the prefrontal cortex, Addict. Biol. 19 (2014) 612–622, https://doi.org/10.1111/adb.12026.
[35] J.F. Cubells, D.P. van Kammen, M.E. Kelley, G.M. Anderson, D.T. O'Connor, L.H. Price, R. Malison, P.A. Rao, K. Kobayashi, T. Nagatsu, J. Gelernter, Dopamine beta-hydroxylase: two polymorphisms in linkage disequilibrium at the structural gene DBH associate with biochemical phenotypic variation, Hum. Genet. 102 (1998) 533–540.
[36] V. Klimek, G. Rajkowska, S.N. Luker, G. Dilley, H.Y. Meltzer, J.C. Overholser, C.A. Stockmeier, G.A. Ordway, Brain noradrenergic receptors in major depression and schizophrenia, Neuropsychopharmacology 21 (1999) 69–81.
[37] D. Kemali, M. Del Vecchio, M. Maj, Increased noradrenaline levels in CSF and plasma of schizophrenic patients, Biol. Psychiatry 17 (1982) 711–717.
[38] K. Yamamoto, J.F. Cubells, J. Gelernter, C. Benkelfat, P. Lalonde, D. Bloom, S. Lal, A. Labelle, G. Turecki, G.A. Rouleau, R. Joober, Dopamine beta-hydroxylase (DBH) gene and schizophrenia phenotypic variability: a genetic association study, Am. J. Med. Genet. B Neuropsychiatr. Genet. 117B (2003) 33–38.